Effects of Vertical Density Profiles on Bending Properties of Fiberboard with a "Bowl-Shaped" Vertical Density Profile

Yang Zhang
Zhiming Yu

Abstract

To develop bending failure mechanics and establish the bending strength prediction models, fiberboards with both uniform and ''bowl-shaped'' vertical density profiles (VDPs) were manufactured, and their bend loading–deflection relations were evaluated and compared. The bending modulus of elasticity (MOE) and rupture (MOR) of fiberboards with bowl-shaped VDP (BS-fiberboard) were predicted using the sheet laminating theory. The results indicate that when fiberboards are of the same average density, the bending performance of BS-fiberboard is at least 40 percent stronger than uniform fiberboard. The MOE and MOR prediction models of BS-fiberboard correlated with thickness of panel, average density, surface density, density of sandwich layer, and thickness of sandwich layer and had a very strong predictive ability.

Fiberboard is manufactured by a series of production processes, such as fiber separation, fiber treatment, formation, and hot pressing, using plant fibers as the main raw material. Because of its high performance under light structural applications and its low price, fiberboard is widely applied in the areas of light construction, furniture design, etc. It is usually used as wallboard, floor and cement molding board, ceiling, hollow door, furniture board, etc. Fiberboard usually requires a higher strength when used as a building material, and this is often achieved by increasing the average density and the quantity of resin, neither of which can necessarily improve board strength in practice. This is because the performance of the board has been affected by the existence of its vertical density profile (VDP), the density variance of wooden composites through a board's thickness (Kelly 1977, Suo and Bowyer 1994, Dai et al. 2000, Wang and Winistorfer 2000).

The VDP greatly impacts the physical and mechanical performance of wood-based panels (Kelly 1977). Traditional VDPs are usually symmetric along the thickness axis, with higher density on the surface and lower density in the core layer; the highest density usually appears at a certain thickness position from the panel surface. Therefore, the traditional VDP is called M-type VDP due to its M shape.

Wood fiber is a poor conductor of heat. In the process of hot pressing, the adhesive cures gradually and continuously from the surface to the sandwich layer as the mat temperature achieves the target curing temperature from outside to inside. The final density at different positions from the surface depends on the pressure for resin solidification and the inner environment of the mat during hot pressing (Wang and Winistorfer 2000, Zhang and Yu 2009a). Therefore, during the hot pressing of fiberboard, the temperature gradient, moisture gradient, and variation in resin curing level of the inner mat will give an uneven VDP. The precuring layer can be effectively eliminated by water spraying on the surface, and section closure can reduce transition zone thickness and increase sandwich lay density (Zhang and Yu 2009b).

Many earlier theoretical and experimental studies investigated the effects of heat; moisture; orientation of the tracheids, vessels, and fibers; and pressing strategies on the formation of VDP (Plath 1971, Geimer et al. 1975, Geimer 1979), and the effect of VDP shape on product properties (Plath 1971, Suo and Bowyer 1995, Steidl et al. 2003). Other studies focused on modeling the bending modulus of elasticity (MOE) based on layer properties that are affected by VDP (Plath 1971, Kelly 1977, Carll and Link 1988, Dai

The authors are, respectively, Lecturer and Professer, Dept. of Wood Sci. and Technol., Beijing Forestry Univ., Beijing, People's Republic of China (zhangyang042002@yahoo.com.cn, yuzhiming@bjfu.edu.cn [corresponding author]). This paper was received for publication in April 2011. Article no. 11-00055.

Forest Prod. J. 61(7):510–516.

et al. 2000, Wang and Winistorfer 2001, Jin et al. 2009). These studies have greatly contributed to the understanding, and hence the manipulation, of the VDP for minimizing overall panel density in practice. The existence of a precuring layer can degrade the bending performance and surface quality of panels, as well as the strength–weight ratio.

With regard to bending performance, many research studies have focused on MOE and modulus of rupture (MOR) as the most important mechanical indexes of fiberboard, and several predictive models have been established (Jin et al. 2009, Zhang and Yu 2009a). In this study, the VDP distribution in fiberboards were optimized and designed based on theories of material mechanics; ''bowl-shaped'' VDP fiberboard was designed by means of eliminating the precuring layer and reducing the differences in VDP distribution. To improve the material utilization ratio and performance controllability, predictive models of MOE and static bending strength of fiberboard were established based on sheet laminating theory.

Materials and Methods

Raw materials

The fiber, phenol–formaldehyde liquid resin, and emulsified wax used in the studies were from a fiberboard mill located in Beijing that primarily uses a mixture of hardwood fiber.

The solid loading levels of resin and wax were 3.5 and 0.5 percent, respectively, based on the ovendry weight of the fiberboard. According to the moisture content of each batch of dry fibers, water was added to keep the target moisture content at 8 percent for each mat.

Board fabrication

Two sets of fiberboards, fiberboards with uniform VDP (U-fiberboard) and fiberboards with bowl-shaped VDPs (BS-fiberboard), were fabricated by changing two selected variables: board density and board structure (either with U-fiberboard or BS-fiberboard). Compared with fiberboard with conventional M-shaped density profiles (C-fiberboard), BS-fiberboard did not have a precured layer. The thickness of the surface layer in BS-fiberboard was thinner, and the density profile of the inner layer in BS-fiberboard was flatter.

BS-fiberboard.—The nominal density levels of BS-fiberboard ranged from 550 to 850 kg/m^3. To produce BS-fiberboard, a special pressing cycle, which was similar to a ''high-low-high'' hot-pressing curve, and a humidifying treatment for the surface of mats were used (Jin et al. 2009, Zhang and Yu 2009b). The surface of the mats was conditioned using a humidifying treatment, and the mats were then moved to the hot press and pressed under the conditions shown in Table 1.

U-fiberboard.—The nominal density levels of U-fiberboard ranged from 500 to 1,000 kg/m^3 at an interval of 100 kg/m^3, resulting in six target density levels. To produce fiberboard with uniform VDP through the board thickness, a special predetermined warm prepressing cycle, which was similar to the previously reported cold-pressing method, was used (Geimer et al. 1975, Geimer 1979, Wang and Winistorfer 2001, Jin et al. 2009). All mats were prepressed to the target thickness of 12 mm at a platen temperature of 70°C and then held at the target thickness until the core temperature reached the platen temperature. Subsequently, both the top and bottom platens were heated to 170°C. The boards were removed as soon as the core temperature reached 125°C. The whole pressing cycle ranged from 20 to 25 minutes depending on the board density, with denser boards requiring more time.

Specimen preparation and testing.—The pressed strand boards were trimmed to 533 by 533 mm and then conditioned for 1 week in a standard conditioning climate of 20°C and 65 percent relative humidity before being cut into test specimens. For each board, six 50 by 50-mm specimens were prepared for VDP determination, and four 75 by 317-mm specimens were cut for bending tests. Prior to testing, all the specimens were further conditioned under the same standard conditioning climate until they were equilibrated. CreCon's X-ray densitometer was used to measure the VDP of fiberboard specimens. The tests for other properties were conducted according to standard CSA O437.1-93 (ASTM International 2004). The weight and dimension (i.e., thickness, width, and length) of each specimen were measured to calculate its actual density.

The average value of each property and the corresponding average density of the specimens cut from the same board were used to derive the regression equations and to plot the density–property correlation curves shown in Figures 1 through 6.

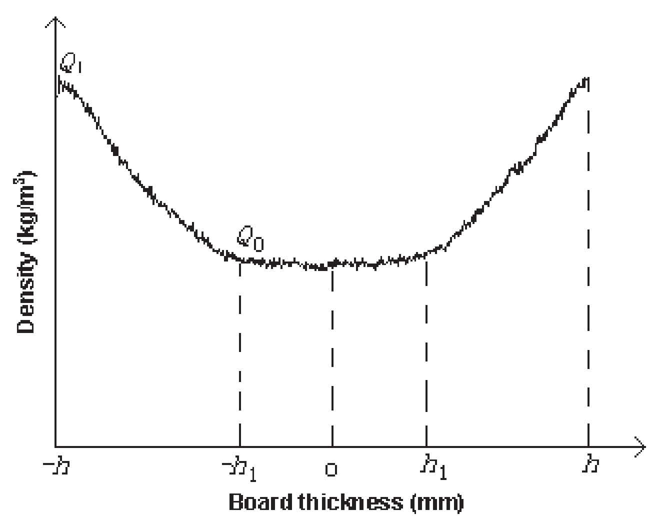

Figure 1.—Vertical density profile (VDP) of uniform VDP fiberboard with different densities.

Table 1.—Hot pressing conditions for bowl-shaped fiberboard.

Hot pressing temp (°C)	Rise time (s)	High pressure (MPa)	Holding time at high pressure (s)	Low pressure (MPa)	Holding time at low pressure (s)
180	20	3	90	1	330

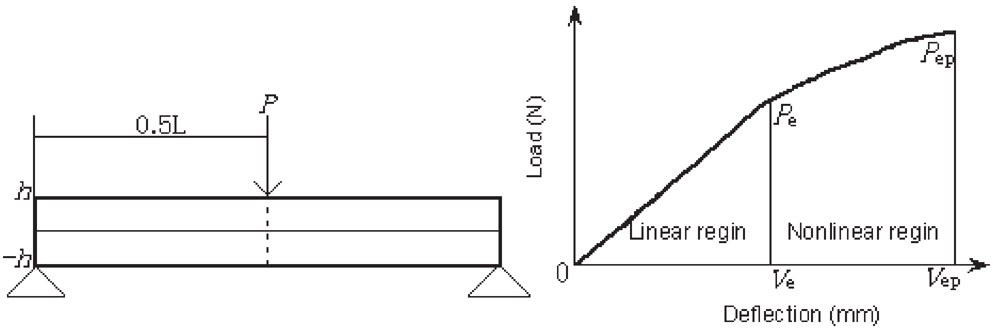

Figure 2.—Vertical density profile (VDP) of bowl-shaped VDP fiberboard with different densities.

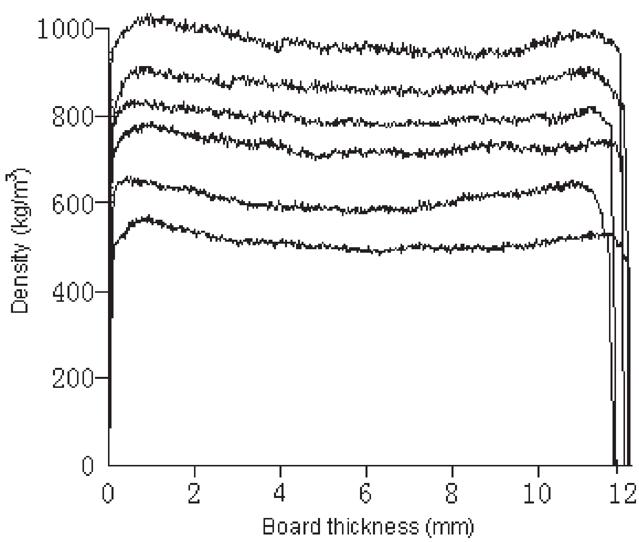

Figure 3.—Load–deflection relation curve of uniform fiberboard.

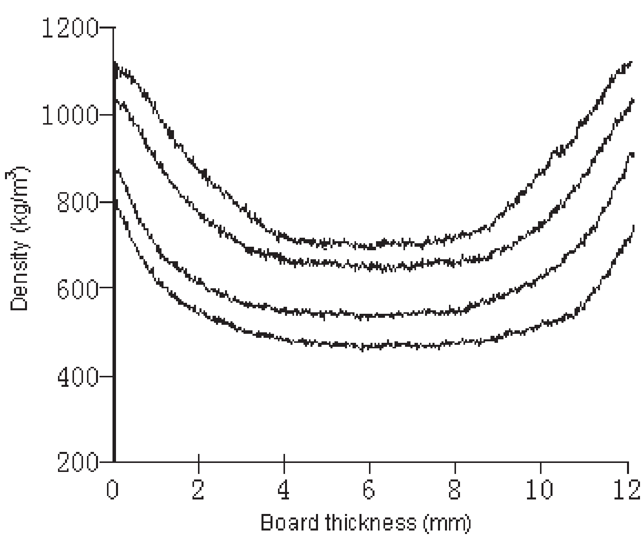

Figure 4.—Load–deflection relation curve of bowl-shaped fiberboard.

Derivation of Prediction Model

In the process of three-point load bending, upper surface in compression, and lower surface in tension, an external

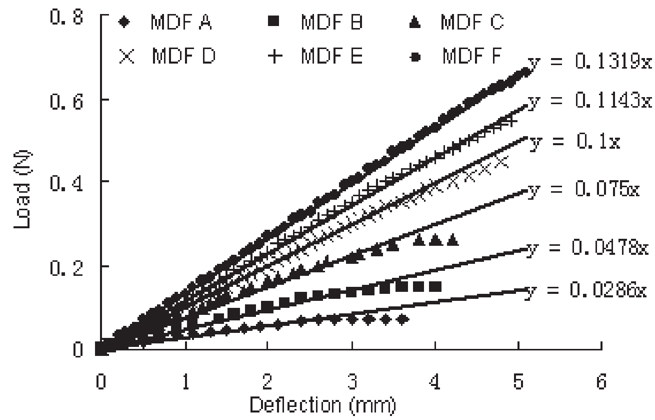

Figure 5.—Relation of modulus of rupture and modulus of elasticity with density of uniform fiberboard.

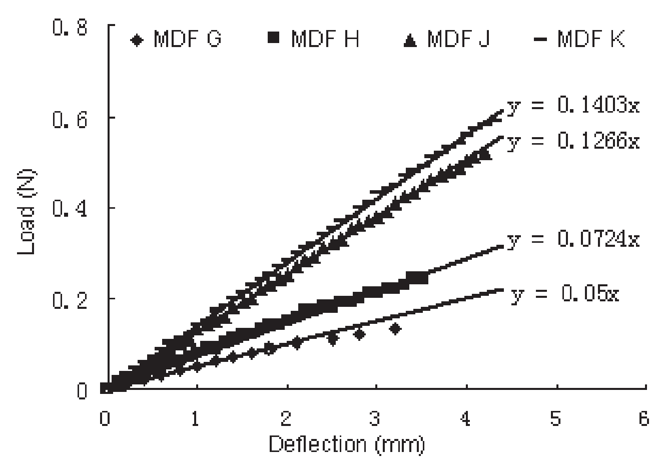

Figure 6.—Relation of failure deflection with average density of fiberboard.

load acts on the middle cross section of fiberboard; therefore, it suffers the highest moment of flexure and generates the highest stress. Bending failure usually appears in this cross section. To simplify the research, fiberboards were considered to be folded together by numerous isotropic sheets of tiny thickness. The theory of sheet folding was introduced to study bending performance of fiberboard.

Conditions for model deduction

The conditions for model deduction are as follows:

1. bonded connectivity between adjacent fibers in fiberboard, namely, continuity hypothesis;
2. tiny load speed of bend loading, keeping panels in the balanced state on each loading, namely, pure bending hypothesis;
3. tiny deformation compared with panel thickness, that is, tiny deformation hypothesis;
4. fiberboard divided into countless sheets along the thickness direction via differential calculus, the mechanical property of every single sheet depending on density.

$$\mathrm{MOE} = f(Q) \tag{1}$$

$$P_{\mathrm{ep}} = F(Q) \tag{2}$$

$$V_{\mathrm{ep}} = G(Q) \tag{3}$$

where MOE is the modulus of elasticity (MPa), P_{ep} is the failure load (N), and V_{ep} is the failure deflection (mm);
5. before and after bending deformation, each sheet parallels the neutral panel, meanwhile there is no length modification;
6. toward the sheet, the vertical component of stress is far smaller than the horizontal inner component of stress, and the stress only acts on the inside of each sheet;
7. other facts are equal, e.g., wood fiber, glue, resin usage, panel moisture.

Characteristic and quantized model of BS-fiberboard

Figure 7 shows the BS-fiberboard made by this technology, with the highest density appearing at coordinates (h, Q_1) and ($-h$, Q_1). The coordinates of the lowest density of the mat, which were in the middle position, were (0, Q_0). In consequence, thickness at ($-h$, $-h_1$) or (h_1, h) can be defined as the upper or lower surface, and thickness between ($-h_1$, h_1) was the sandwich layer. VDP of the surface was the upward quadratic parabola, while VDP of the sandwich layer was uniform. So, VDP of fiberboard can be described piecewise by the quadratic function:

$$Q = \begin{cases} a(y-b)^2 + c & -h \le y \le -h_1 \\ Q_0 & -h_1 \le y \le h_1 \\ a(y+b)^2 + c & h_1 \le y \le h \end{cases} \tag{4}$$

where a, b, and c are undetermined coefficients of quadratic function separately, y is the thickness value of the VDP, and Q is the density value of the VDP.

In terms of dots on quadratic parabola of (h, Q_1) and (h_1, Q_0), the solution formula of a, b, and c can be concluded:

$$\begin{cases} a(h-b)^2 + c = Q_1 \\ a(h_1-b)^2 + c = Q_0 \\ Q_0 h_1 + \int_{h_1}^{h} \left[a(y-b)^2 + c\right] dy = Q_{\mathrm{A}} h \end{cases} \tag{5}$$

Consequently, the characteristic and quantized model of BS-fiberboard VDP was the function involving surface density (Q_1), sandwich layer density (Q_0), thickness (h_1), and average density (Q_{A}) of the panel.

Bend loading–deflection curve of fiberboard

Figure 8 indicates that the upper surface was in compression and the lower surface was in tension when fiberboard was under three-point bending (Steidl et al. 2003, Zhang and Yu 2009a). Exterior loading acted on the middle cross section of the panel, which suffered the largest bending moment and generated the highest stress; bending failure usually occurred in this section. Therefore, the middle cross section was the focus of this study. As Figure 8 shows, based on the relation curve between bend loading and deflection, the bending process of the panel can be divided into two stages, linear bending and nonlinear bending.

When loading was lower than ultimate load (P_{e}), a directly proportional relationship appeared between bend deflection (V) and loading (P). All sheets of the panel were under a state of elastic bending, which resulted in a relation equation of bend loading and deflection:

$$P = \frac{P_{\mathrm{e}}}{V_{\mathrm{e}}} V \tag{6}$$

When loading was greater than ultimate load P_{e}, it was in a nonlinear bending state for the panel and the gradient between loading and deflection became gradually smaller.

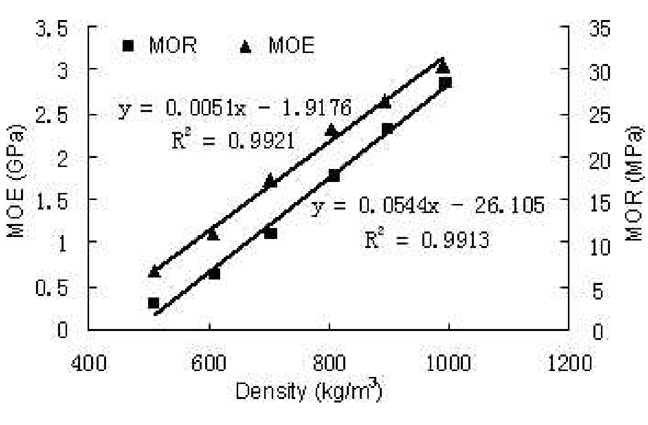

Figure 7.—Vertical density profile curve of bowl-shaped fiberboard. MOE = modulus of elasticity; MOR = modulus of rupture.

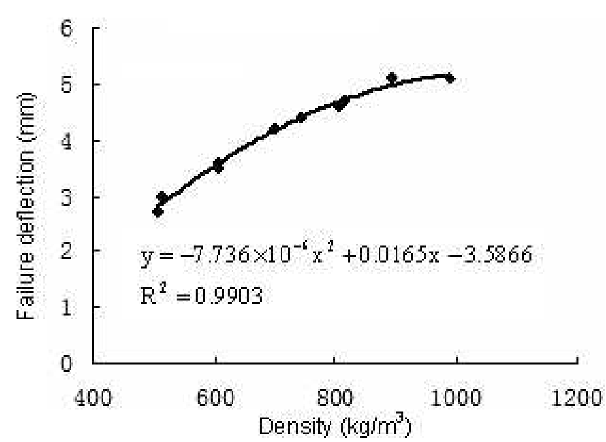

Figure 8.—Relationship between loading and deflection in three-point load bending process of fiberboard.

When loading reached its failure load (P_{ep}), the panel was damaged. The relation equation of loading and deflection was now in this state:

$$P = g(V) \tag{7}$$

As the gradient of the relation curve between loading and deflection became lower in the nonlinear region, a new relation model was drawn:

$$g'(V) \leq \frac{P_e}{V_e} \quad \text{and} \quad g''(V) \leq 0 \tag{8}$$

The impact model of VDP on MOE

MOE of fiberboard is the MOE of the linear relation area between bend deflection and loading in the process of three-point load bending (Jin et al. 2009, Zhang and Yu 2009a). The formula is

$$\text{MOE}_T = \frac{L^3}{4Bs^3}\frac{\Delta P}{\Delta V} = \frac{L^3}{4Bs^3}\frac{P_e}{V_e} \tag{9}$$

where ΔP is the linear load differenc under proportional limit, ΔV is the linear deflection differenc under proportional limit, L is the span length between two bearings (mm), B is the sample width (mm), and s is the sample thickness.

Since the density along thickness direction is different for non–U-fiberboard, the MOE is different as well (Dai et al. 2000, Steidl et al. 2003, Jin et al. 2009, Zhang and Yu 2009a). The result of MOE coming from Equation 9 is the one for whole panel, which also has positive correlation with the gradient of relation curve of bend loading and deflection.

In the linear area between bend loading and deflection, any point along the cross section of the fiberboard demonstrates a Hooks' law relationship (Jin et al. 2009, Zhang and Yu 2009a):

$$\sigma(y) = \text{MOE}\frac{y}{\rho} = f(Q)\frac{y}{\rho} \tag{10}$$

where ρ is the radius of the curvature of the middler layer in the bending process.

In terms of statics, the sum of the normal stress of each point on the panel cross section is 0, the sum of the force moment of each point equals the external one, and the equations are from Jin et al. (2009) and Zhang and Yu (2009a):

$$\int_A \sigma \, dA = B\int_{-h}^{h} \sigma \, dy = 0 \tag{11}$$

$$\int_A \sigma y \, dA = B\int_{-h}^{h} \sigma y \, dy = M_1 \tag{12}$$

where M_1 is moment of couple (N·mm).

Substituting Equation 10 for 12, then

$$\int_{-h}^{h} f(Q)y^2 \, dY = M_1\rho/B \tag{13}$$

To hypothesize equivalent bending modulus of elasticity of the panel for MOE_P, Equation 14 can be obtained from Equation 12:

$$\text{MOE}_P \int_{-h}^{h} y^2 \, dY = M_1\rho/B \tag{14}$$

Equation 15 can be drawn from Equations 13 and 14:

$$\text{MOE}_P = \frac{3\int_{-h}^{h} f(Q)y^2 \, dy}{h^3} \tag{15}$$

The prediction model of modulus of bending elasticity of the fiberboard can be obtained from Equations 4 and 15.

The impact model of VDP on MOR

MOR means bending intensity of the panel, expressed according to Steidl et al. (2003), Jin et al. (2009), and Zhang and Yu (2009a):

$$\text{MOR}_T = \frac{3L}{2B \cdot s^2}P_{ep} \tag{16}$$

Based on Equation 16, under conditions of a fixed span, panel width, and thickness, there is a direct proportional relationship between MOR and failure load P_{ep}.

The prediction model of MOR has been a key difficulty in fiberboard research. In terms of bending performance of BS-fiberboard (i.e., the first strength theory and second strength theory), we investigated the MOR prediction model of fiberboard in this study. Because BS-fiberboard was brittle material (shown as follows), the reason of strength failure resulted from fracture destruction, which can be divided into two circumstances: maximum tensile stress and maximum tensile strain.

When the maximum tensile strength resulted in strength failure, the dangerous area of fracture destruction of the BS-fiberboard was regarded as the panel surface, according to P_{ep}, which is tolerable for the surface. The MOR_{PP} (based on maximum stress theory) can be calculated by Equations 2 and 16:

$$\text{MOR}_{PP} = \frac{3L}{2B \cdot s^2}P_{ep} = \frac{3L}{2B \cdot s^2}F(Q_1) \tag{17}$$

When the maximum tensile strain produced failure, the failure load of BS-fiberboard was generated while the bending deflection of the whole panel reached tolerable failure deflection (V_{ep}). The MOR_{PV} can be obtained from Equations 3, 9, and 16:

$$\text{MOR}_{PV} = \frac{6s}{L^2}G(Q_A)\text{MOE}_P \tag{18}$$

Where minor values of MOR_{PP} or MOR_{PV} were the MOR prediction value (MOR_P) of fiberboard:

$$\text{MOR}_P = \min(\text{MOR}_{PP}, \text{MOR}_{PV}) \tag{19}$$

Results and Discussion

VDP structural equation of fiberboard

Figure 1 indicates that the VDP structural equation of U-fiberboard with different average densities is a constant function. Figure 2 indicates that the VDP structural equation of BS-fiberboard with different average densities is a nonlinear function. Combined with all values of VDP quantized factors from Figures 1 and 2, the VDP quantized factors of panels, i.e., *a, b, c,* h_1, Q_0, can be calculated through Equations 2 and 3 (Table 2).

Comparison of bending performance between BS-fiberboard and U-fiberboard

Based on the findings shown in Figure 3 of the relation curve of bend loading–deflection of U-fiberboard, the gradient has a positive correlation with density in the linear area with an average density from 500 to 1,000 kg/m^3. The higher the density, the worse the bend failure loading of the panel was. When the average density ranged from 500 to 800 kg/m^3, an obvious nonlinear area appeared in the relation curve of bend loading–deflection of U-fiberboard. The proportion of the nonlinear area shrunk as density became higher. When the average density reached 800 to 1,000 kg/m^3, bend loading showed a linear relation with deflection, but no obvious nonlinear area was observed. U-fiberboard was a brittle material. Since the VDP of U-fiberboard was almost flat, the U-fiberboard may have similar properties along its thickness direction under our specific conditions. Therefore, the different densities of fiberboard displayed different bending performance; the lower density boards were elastic plastic materials, while the higher density boards were brittle materials.

Based on the analysis shown in Figure 4, the bend loading–deflection of BS-fiberboard showed a linear relationship when the average density was between 546 to 842 kg/m^3, and a brittle failure occurred. Thus, the BS-fiberboard can be categorized as a brittle material.

Comparing the flexural loading–deflection relation curve of fiberboard B and fiberboard H whose densities were about 600 kg/m^3, it was shown that the BS-fiberboard increased the MOE and MOR by 40 percent under the same average density, and the surface density of the BS-fiberboard was far beyond the average density. After analyzing the stress distribution of flexural loading of the fiberboard, the bottom surface of the fiberboard had the most stress. In the pure bending process, bending properties were controlled by fiberboard surface density. Because the surface density of BS-fiberboard usually exceeded more than 40 percent of the average density, the VDP of BS-fiberboard reflected the corresponding 40 percent increase in MOR and MOE compared with the U-fiberboard.

MOR and MOE prediction model of BS-fiberboard

As shown in Figure 5, the average density of the various U-fiberboards had a linear relationship with MOE and MOR. Therefore, under conditions of uniform moisture, glue and resin usage, etc., the relation equation between density and MOE is as follows:

$$\mathrm{MOE} = f(Q) = 0.0051Q - 1.9176 \tag{20}$$

$$F(Q) = \frac{2b \cdot s^2(0.0544Q - 26.105)}{3L} = \frac{1.3056Q - 626.52}{1,000} \tag{21}$$

Combining Equations 15 and 20, the MOE prediction model of BS-fiberboard was

$$\mathrm{MOE_p} = \frac{3}{500h^3}[1.02a(h^5 - h_1^5) - 2.54ab(h^4 - h_1^4) + 1.7(ab^2 + c)(h^3 - h_1^3) + 1.7Q_0h_1^3 - 639.2h^3] \tag{22}$$

Table 2.—Vertical density profile quantized factors for different bowl-shaped fiberboards.

Panel	Training data					Predicting data		
	Thickness of panel (mm)	Average density (kg/m^3)	Surface density (kg/m^3)	Density of sandwich layer (kg/m^3)	Thickness of sandwich layer (mm)	*a*	*b*	*c*
A	6	509	—	—	—	—	—	—
B	6	608	—	—	—	—	—	—
C	6	701	—	—	—	—	—	—
D	6	805	—	—	—	—	—	—
E	6	893	—	—	—	—	—	—
F	6	989	—	—	—	—	—	—
G	6	546	805	476	1.18	20.1	0.08	122
H	6	615	889	547	1.92	17.6	0.03	252
J	6	745	1037	652	2.55	15.9	0.04	461
K	6	842	1104	703	2.14	19	0.01	420

Table 3.—Comparison of calculated values and actual values, which are from modulus of elasticity (MOE) and modulus of rupture (MOR) of bowl-shaped fiberboard.[a]

Panel	$\mathrm{MOE_P}$ (GPa)	$\mathrm{MOE_T}$ (GPa)	K_{MOE} (%)	$\mathrm{MOR_P}$ (MPa)	$\mathrm{MOR_T}$ (MPa)	K_{MOR} (%)
G	1.09	1.16	−6.03	5.71	5.42	5.35
H	1.81	1.68	7.73	10.88	10.01	8.69
J	3.02	2.93	8.01	20.94	21.67	−3.36
K	3.32	3.25	2.15	27.19	25.42	6.96

[a] $\mathrm{MOE_P}$ = the prediction value of MOE; $\mathrm{MOR_P}$ = the prediction value of MOR; $\mathrm{MOE_P}$ = the test value of MOE; $\mathrm{MOR_P}$ = the test value of MOR; $K_{\mathrm{MOE}} = (\mathrm{MOE_P} - \mathrm{MOE_T})/\mathrm{MOE_T}$; $K_{\mathrm{MOR}} = (\mathrm{MOR_P} - \mathrm{MOR_T})/\mathrm{MOR_T}$.

From Figure 6, the average density of various fiberboards can be seen to have had a nonlinear relationship with failure deflection. Therefore, under conditions of uniform moisture, glue and resin usage, etc., the relation equation between average density and failure deflection can be concluded as follows:

$$V_{ep} = G(Q_A) = -7.736 \times 10^{-6} Q_A^2 + 0.0165 Q_A - 3.5866 \quad (23)$$

MOR prediction model of BS-fiberboard can be concluded via Equations 17, 18, 19, 21, and 23.

Table 3 provides a comparison of the calculated values and the actual values, which were from MOE and MOR of BS-fiberboard separately; their differential values were less than 9 percent. As a result, the prediction models of MOE and MOR, established by this study, provide very strong predictive ability.

Conclusions

Within the materials, parameters, and methods examined in this study, the main conclusions were as follows:

- Bending performance of fiberboards with different densities or VDP types had tremendous variability. The U-fiberboard with a density lower than 800 kg/m^3 can be categorized into a plastic material; an obvious plastic area appears in the loading–deflection curve of the bending process. The plastic area becomes smaller as the density increases. When density was higher than 800 kg/m^3, the U-fiberboard was regarded as a brittle material. BS-fiberboard that had a density higher than 550 kg/m^3 was considered a brittle material. Under the situation in which both U- and BS-fiberboards had the same average density, the bending performance of BS-fiberboard was at least 40 percent stronger than U-fiberboard.
- Based on the sheet laminating theory and a simulated model of the VDP, the established MOE and MOR prediction model of BS-fiberboard displayed good predictive ability, which obtained MOE and MOR values close to the actual ones.
- Under the situation of pure bending failure, the MOR and MOE of BS-fiberboard had a close relationship with VDP factors, which cannot be decided by a single factor alone.

Literature Cited

ASTM International. 2004. Standard test methods for evaluating properties of wood-base fiber and particle panel materials. ASTM D1037-99. ASTM International, West Conshohocken, Pennsylvania.

Carll, C. G. and C. L. Link. 1988. Tensile and compressive MOE of flake boards. *Forest Prod. J.* 38(1):8–14.

Dai, C., C. Yu, and P. Hubert. 2000. Modeling vertical density profile in wood composite boards. *In:* Proceedings of the 5th Pacific Rim Bio-Based Composites Symposium, December 2000, Canberra, Australia; Australian National University, Canberra. pp. 220–226.

Geimer, R. L. 1979. Data basic to the engineering design of reconstituted flakeboard. *In:* Proceedings of 13th International Particleboard/Composites Materials Symposium, April 3–5, 1979, Pullman, Washington; Washington State University, Pullman. pp. 105–125.

Geimer, R. L., H. M. Montrey, and W. F. Lehmann. 1975. Effects of layer characteristics on the properties of three layer particleboard. *Forest Prod. J.* 25(3):19–29.

Jin, J. W., C. P. Dai, W. E. Hsu, and C. M. Yu. 2009. Properties of strand boards with uniform and conventional vertical density profiles. *Wood Sci. Technol*. 43:559–570.

Kelly, M. W. 1977. Critical literature review of relationships between processing parameters and physical properties of particleboard. USDA Forest Service, Forest Product Laboratory, Madison, Wisconsin.

Plath, E. A. 1971. Contribution on particle board mechanics. *Holz Roh-Werkst*. 29(10):377–382.

Steidl, C. M., S. Wang, R. M. Bennett, and P. M. Winistorfer. 2003. Tensile and compression properties through the thickness of oriented strand board. *Forest Prod. J*. 53(6):72–80.

Suo, S. and J. Bowyer. 1994. Simulation modeling of particleboard density profile. *Wood Fiber Sci*. 26(3):397–411.

Suo, S. and J. Bowyer. 1995. Modeling of strength properties of structural particleboard. *Wood Fiber Sci*. 27(1):84–94.

Wang, S. Q. and P. M. Winistorfer. 2000. Fundamentals of vertical density profile formation in wood composites. Part 2. Methodology of vertical density formation under dynamic conditions. *Wood Fiber Sci*. 32:220–238.

Wang, S. Q. and P. M. Winistorfer. 2001. Step-closing pressing of medium density fiberboard. Part 1. Influences on the vertical density profile. *Holz Roh- Werkst*. 59:19–26.

Zhang, Y. and Z. M. Yu. 2009a. Effects of hot-pressing parameters on vertical density profile of fiberboard. *J. Beijing Forestry Univ*. 31(4): 118–122.

Zhang, Y. and Z. M. Yu. 2009b. Forecasting model of MOE of fiberboard. *J. Beijing Forestry Univ*. 31(S1):127–130.